Extremely large-stroke hair artificial muscles with fast recovery prepared by a facile and green method

Qian-Ru Xiao[1], Peng Xu[1], Si Sun[1], Xiao-Li Qiang[1], and Xiao-Long Shi[1]

[1]Affiliation not available

January 16, 2023

Abstract

Artificial muscles with large strokes are of special interest in diverse fields. However, it is difficult for large-diameter muscles to be rapidly cycled. In this study, hair artificial muscles with extremely large tensile stroke and fast recovery were prepared simply by twist insertion, coiling and steaming. The maximum tensile stroke for the hair artificial muscles upon water actuation was as large as 10000% and the large-stroke muscles could recover fast in ethanol. With a diameter of 7 mm and a twist density of 2500 turns m^{-1}, the compacted heterochiral hair artificial muscle could elongate 100 times of its original length in water and returned to its initial length in ethanol within 10 s. In addition, these hair artificial muscles maintained their excellent performance after either 100 water-ethanol stimulation cycles or staying in open air for 5 months. Moreover, the hair artificial muscle was able to contract by 59% when lifting 10 times its own weight, pull a wheel model or climb a long distance under water and work as a smart water-sensitive switch. This work demonstrates a facile and green strategy to prepare advanced natural fiber-based artificial muscles that have promising applications in soft robotics and biomedical engineering.

Corresponding author(s) Email: sunsi@gzhu.edu.cn (Dr. Si Sun), qiangxl@gzhu.edu.cn (Dr. Xiao-Li Qiang), & xlshi@gzhu.edu.cn (Dr. Xiao-Long Shi)

Introduction

Artificial muscles that can actively contract, expand or rotate when stimulated by electricity, light, heat, or solvent have drawn considerable attention owing to their potential applications in smart devices and soft robotics[1-3]. Among various types of developed artificial muscles, twisted fibers have drawn considerable attention due to their reversible tensile actuations upon volumetric expansion and similarity to the biological muscle in form[4-6].

For the past decades, a wide range of actuating materials have been used for twisted fiber based artificial muscles, including shape memory materials[7, 8], carbon nanotube (CNT) yarns[9-12], graphene oxide fibers[13, 14], polymers[15, 16], silk[17-19], and hair fibers[20]. CNT yarns can deliver large strokes when stimulated by heat, electricity, or solvent. For instance, a helical fiber actuator from CNT can respond to organic solvents with a tensile contraction of 60% while a self-sensing coaxial CNT based muscle fiber can maintain a ˜11% tensile stroke between electrothermal stimulation and solvent adsorption[21, 22]. Despite the advantages, the high cost of CNT limits its scalable fabrication and practical applications. Inexpensive polymer fibers like polyethylene and nylon fishing lines have also been developed into artificial muscles[23]. The extreme twisting technology caused coiling of the polymer fiber and dramatically amplified the tensile stroke. Nevertheless, it is also demonstrated that the coiling of twisted fibers with a mandrel can obtain larger stroke than that caused by the extreme twist insertion.

In addition to the synthetic materials, there is also a growing need for artificial muscles from natural biocompatible and biodegradable materials. Silk is one of the most impressive natural materials due to its hierarchical structure and superior mechanical properties. A humidity-driven artificial muscle prepared by

coiling and thermal setting of the twisted silk fibers could contract by 70% in about 1 min when the ambient humidity changed from 20% to 80%[19]. Another natural fiber material, human hair, has also been developed into tether-free tensile artificial muscles by disulfide cross-linking[20]. When the twist density of the hair fiber was 3000 turns m^{-1} and the spring index was 15.8, the hair muscles exhibited the best performance, with 94% contraction for the homochiral and 3000% extension for the heterochiral. However, either the acquisition of the dual-filament silk fibers or the chemical crosslinking adds the complexity of the muscle fabrication and artificial muscles with stroke up to 10000% have not been reported so far.

In this study, long human hair was successfully transformed into highly reversible, tether-free, solvent-driven artificial muscles with extremely large tensile stroke and fast recovery by a simple two-step method, namely, twist insertion followed by a coiling and steaming process. Leaving out the chemical reduction and oxidation of the disulfide bonds of the hair, the method adopted here is not only simple and cost-effective, but also environmentally friendly. By simply adjusting the twist density and the diameter of the coiled hair muscles, a tensile stroke of as large as 10000%, more than 3 times of the largest stroke reported so far, was achieved upon stimulation. Meanwhile, ethanol could significantly shorten the recovery time of the artificial muscle to merely 10 seconds. Moreover, the hair artificial muscles were also demonstrated for weight-lifting, climbing, and sensitively control the switch of a circuit.

Materials and Methods

Materials

Ethanol was purchased from Sinopharm Chemical Reagent Co., Ltd. Pure water was provided by the water purification systems (Direct-Q8UV-R, Merk Millipore, Germany). Human hair was provided by the author Qian-Ru Xiao, who has no objection to the hair being used in this study.

Preparation and characterization of the twisted hair fibers

Long black hair with a diameter of 90-100 μm was cleaned and used in this study. The length of the hair fibers ranges from 40 to 70 cm. For preparation of the twisted hair fiber, a raw hair fiber was placed vertically with a weight hanging on its bottom end. Twist was inserted at the top end of the hair fiber by a motor in the counter-clockwise direction. Meanwhile, the weight at the bottom was tethered to avoid twist release during the twist insertion. After twisting, the fiber was folded at its middle point and formed a torque-balanced two-plied structure. Then the single twisted hair filament was attached to a folded paper with an observation window and observed with a macro lens. ImageJ was used to measure the helical angles.

Preparation and characterization of the tensile hair artificial muscles

For preparation of the tensile hair artificial muscles, the obtained twist-stable double-plied hair fibers were wrapped around cylindrical mandrels of different diameters tightly in clockwise and counterclockwise directions respectively with both ends tethered. After steaming for 30 min, the coiled hair muscles were untied from the mandrel and relaxed in the open air. The fully relaxed hair muscles were observed with a macro lens and imageJ was used to measure the coil pitch. Differential scanning caborimetry spectra (DSC) for pristine hair fibers, hair fibers heated for 30 min, and hair fibers steamed for 30 min were obtained on a TA differential scanning caborimetry (USA, Q2000).

Muscle actuation test

The actuation performance of both homochiral and heterochiral hair artificial muscles with different diameters and different twist densities were characterized under water. Then the actuated hair muscles were put into ethanol for recovery. Digital camera was used to record the video of the real-time actuation process.

The tensile stroke of the hair artificial muscles was calculated. In addition, both the homochiral and heterochiral muscles were put into water and ethanol repeatedly for 100 times to test their reversibility. And the actuation performance of both the homochiral and heterochiral hair muscles was investigated after 5 months to test their stability.

Applications of the hair artificial muscles

Homochiral hair artificial muscles with the spring index of 8 and twist density of 2500 turns m^{-1} were used for weight lifting, pulling a model of car wheels under water, and sensitively switch off the light emitting diodes (LEDs) when exposed to water. The heterochiral hair muscles with the spring index of 15 and twist density of 2500 turns m^{-1} was used as a "sea cucumber" for climbing along a barbed cord under water.

Results and Discussion

Fabrication and characterization of the twisted hair fibers

A facile two-step method combining twisting and steaming was used to fabricate the hair artificial muscles. The fabrication process is schematically illustrated in **Figure 1** .

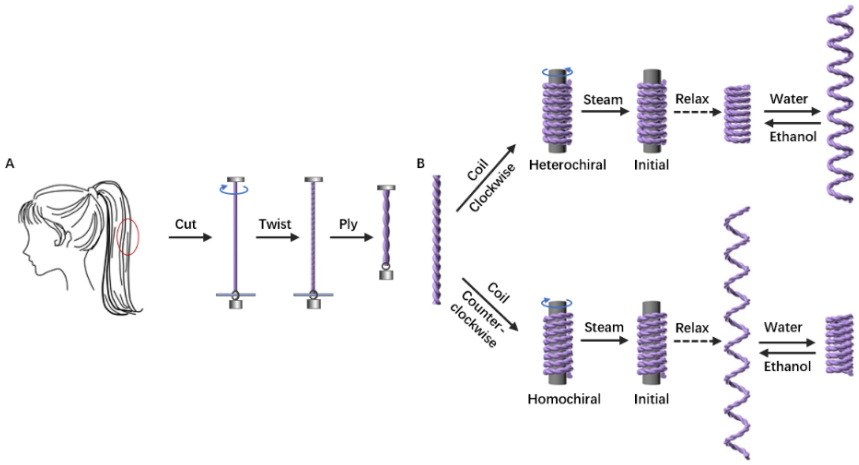

Figure 1 Schematic illustration of the fabrication process of **(A)** a torque-balanced two-plied hair fiber and**(B)** heterochiral and homochiral hair artificial muscles and the solvent-driven actuation.

First, a certain length of human hair was hanged vertically with a load torsionally tethered, and twisted counter-clockwise with a motor for some time (**Figure 2A**). By adjusting the twisting time, hair fibers with different twist densities (1000, 1500, 2000, 2500, 2650 turns m^{-1}) were obtained. The morphology of these hair fibers was examined with a micro lens and shown in **Figure2B** . It can be seen that the longitudinal elements changed from straight to helical after twisting and their angular displacement increased with the increase of the twist density. The helical angles can be approximated with the following equation:

$$\alpha = (2\pi rT)$$

where r is the radial distance from the center of the hair fiber (˜100 μm), and T is the amount of inserted twist divided by the length of the hair fiber. In addition to the theoretical value, image J was also used

to measure the actual helical angles of these fibers. It can be seen from the graph in **Figure 2C**that the measured values of these angles agree well with the calculated values.

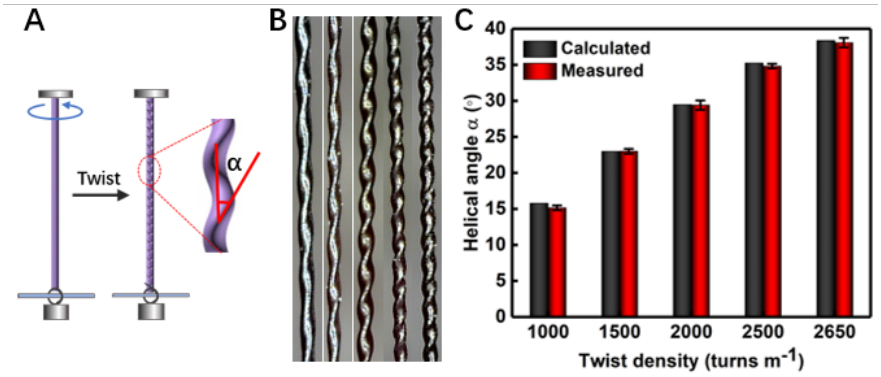

Figure 2 (A) Illustration of measuring the helical angles of the twisted hair fiber. **(B)** The morphology of the twisted hair fibers with the twist density of 1000, 1500, 2000, 2500, 2650 turns m^{-1}. **(C)** The calculated and measured helical angles of the hair fibers with twist density of 1000, 1500, 2000, 2500, 2650 turns m^{-1}.

Fabrication and characterization of thehair artificial muscles

After twisting, the torsional stress generated during the twist insertion tends to cause twist release of the hair fiber when the torsional tethering is removed. To balance the strong untwisting torque, the hair fiber was folded at its middle point and plied together to achieve a self-balanced structure (**Figure 3A**). When the twist density was less than 1000 turns m^{-1}, the self-plied fiber was too loose at the end. Whereas inserting more than 2650 turns m^{-1} of twist into the hair fiber would cause the fiber to break during twisting. Therefore, twist densities of 1000, 1500, 2000, 2500, and 2650 turns m^{-1} were used for the following experiment. The torque-balanced two-plied hair fibers were then wrapped tightly around cylindrical mandrels clockwise or counterclockwise and steamed for 30 min. When the direction of the fiber twist matches the coil's wrapping direction, the obtained coiled muscles are referred to as homochiral artificial muscles. On the other hand, when the direction of the fiber twist and the coil's wrapping direction are opposite, the obtained coiled muscles are referred to as heterochiral artificial muscles. The diameter of the mandrel was 1.6, 3.0, 5.0, 7.0, and 8.0 mm, respectively. The resulted spring index, which is the ratio of the mandrel diameter to the two-plied hair fiber diameter, was 8, 15, 25, 35, and 40.

After hydrothermal setting, coiled hair artificial muscles were untied from the mandrels and relaxed in the ambient air. The relaxed heterochiral hair artificial muscles and the homochiral muscles have distinct morphology. The coils of the heterochiral hair artificial muscles remained in contact with each other regardless of their diameters (**Figure 3B**), while the coils of the homochiral muscles gradually loosened up (**Figure 3C-i**) and extended to a long thin squiggle shape. For convenience, the diameter of the homochiral hair muscle before relaxation is considered as the homochiral muscle's diameter, and the length before relaxation is considered as the homochiral muscle's initial length, which can be achieved after water actuation (**Figure 3C-ii**). It can be seen from **Figure 3D** that no significant correlation was found between the extension of the homochiral hair muscles and their twist densities. As for the influence of the diameter on the elongation of the homochiral hair muscles, however, it was found that the larger the initial diameter of the muscle, the longer the muscle extended (**Figure 3E, 3F**). Coil pitch, which is the distance between the adjacent muscle coils and denoted as δ, was used to quantitatively analyze the extension of the homochiral artificial muscles (**Figure 3G**). ImageJ was used to measure the coil pitch of the homochiral hair muscles with the diameter of 1.6, 3.0, 5.0, 7.0, and 8.0 mm. The result is shown in **Figure3H** . It can be seen that the coil pitch increases with the diameter of the homochiral muscle. The coil pitch for the fully relaxed homochiral

muscles could be as large as 8 to 9 mm, about 3 times larger than the disulfide crosslinked hair muscle[20]. The elongation and coil pitch of the homochiral hair artificial muscles may provide a structural basis for their lateral actuation performance.

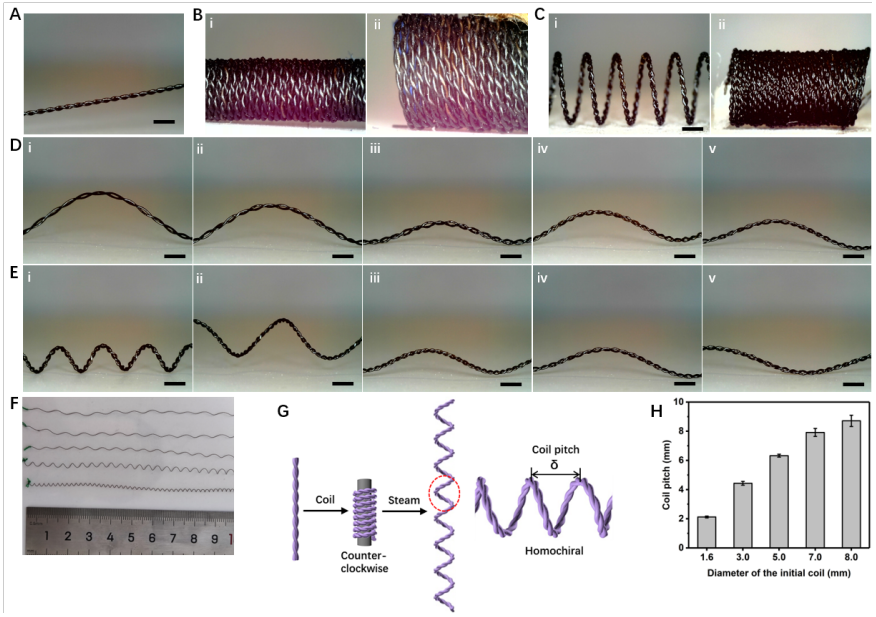

Figure 3 (A) The morphology of the self-balanced two-plied hair fiber. **(B)** The morphology of the heterochiral hair muscles with the spring index of 8 (i) and 15 (ii). **(C)**The morphology of the homochiral hair muscles after being untied from the mandrel (i), and fully contracted in water (ii). **(D)** The morphology of the homochiral hair artificial muscles with the diameter of 7 mm and the twist densities of 1000, 1500, 2000, 2500, and 2650 turns m^{-1}. **(E)** The morphology of the homochiral hair muscles with the twist density of 2650 turns m^{-1} and the diameter of 1.6, 3.0, 5.0, 7.0, and 8.0 mm. **(F)** Digital photos of homochiral hair muscles with the twist density of 2650 turns m^{-1} and the diameter of 1.6, 3.0, 5.0, 7.0, and 8.0 mm. **(G)** Schematic illustration of a homochiral artificial muscle made from a self-balanced two-plied hair fibers and the measurement of the coil pitch δ. **(H)** Measured coil pitch for homochiral hair muscles with the diameter of 1.6, 3.0, 5.0, 7.0, and 8.0 mm. Scale bars for A, C, D, and E: 1 mm.

Actuation performance of the hair artificial muscles

The actuation performance of both the homochiral and heterochiral hair artificial muscles in response to water and ethanol were studied. To investigate the impact of both the twist densities and the spring index of the hair muscles on their actuation performance, homochiral and heterochiral hair muscles with the same twist density but different diameters or with the same diameter but different twist densities were prepared and used for the study.

Results are shown in **Figure 4** . Homochiral hair artificial muscles contract in water and elongate in ethanol (**Figure 4A, Video S1 and S2**), while the heterochiral muscles elongate in water and contract in ethanol (**Figure4B**). **Figure 4C** presents the photos of a homochiral hair muscle with the twist density of 2500 turns $m^{-1}$and the diameter of 7.0 mm at different time points of the actuation process. The muscle was about 235 mm long in the beginning. When activated with water, the hair coils would rotate radially and contract along the axial direction, bringing the coils closer until they were adjacent to each other. After shrinking into a 2 mm tight spring structure, the hair muscle was put into the ethanol to extend. It could quickly rotate radially and extend along the axial direction to 220 mm long in 50 s.

Similarly, the length change of a heterochiral hair muscle with the twist density of 2650 turns m^{-1} and the diameter of 8.0 mm in response to water and ethanol is shown in **Figure4D** . The 1.5 mm long hair muscle extended to 150 mm long in only 32 s in water and shortened back to 1.5 mm long in ethanol within 10 s, exhibiting a very fast response rate to ethanol. As can be seen from**Figure 4E** and **Figure 4F**(**Video S3 and S4**), the actuation was really fast during the first 10 to 20 s, and slowed down later on. The maximum actuation speed could reach 500% s^{-1}. Tensile stroke of both homochiral and heterochiral hair artificial muscles increases with not only the spring index of the helical muscles (**Figure4E, 4F**), but also the twist density of the hair fibers (**Figure 4G, 4H**). Surprisingly, when the twist density reached 2500 turns m^{-1} and the diameter reached 7.0 mm, the tensile stroke was as large as 10000% for either the heterochiral or homochiral hair muscles. Since the homochiral hair muscle extended after untying from the mandrel, the length before extension is considered as its initial length. In addition to the heterochiral hair muscle with the highest twist density and largest diameter, nearly all heterochiral hair muscles could contract to its initial length within 20 s (**Figure 4F, 4H**).

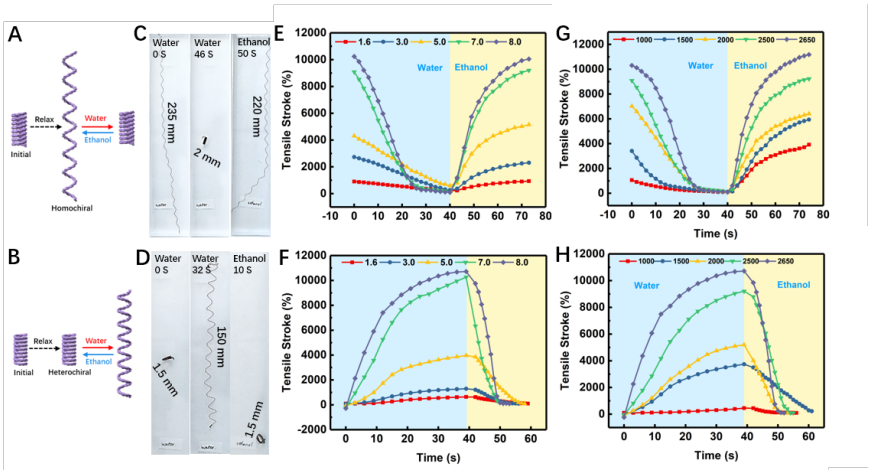

Figure 4 Illustration of the actuation of **(A)**the homochiral and **(B)** the heterochiral artificial muscles in response to solvents. Photographs of **(C)** the homochiral and**(D)** the heterochiral artificial muscles before and after actuation in water and ethanol. **(E)** Tensile stroke of the homochiral artificial muscles with the twist density of 2500 turns m^{-1} and the diameters of 1.6 mm, 3.0 mm, 5.0 mm, 7.0 mm, and 8.0 mm. **(F)** Tensile stroke of the heterochiral artificial muscles with the twist density of 2650 turns m^{-1} and the diameters of 1.6 mm, 3.0 mm, 5.0 mm, 7.0 mm, and 8.0 mm. **(G)** Tensile stroke of the homochiral artificial muscles with the diameter of 7.0 mm and the twist densities of 1000 turns m^{-1}, 1500 turns m^{-1}, 2000 turns m^{-1}, 2500 turns m^{-1}, and 2650 turns m^{-1}. **(H)** Tensile stroke of the heterochiral artificial muscles with the diameter of 8.0 mm and the twist densities of 1000 turns m^{-1}, 1500 turns m^{-1}, 2000 turns m^{-1}, 2500 turns m^{-1}, and 2650 turns m^{-1}.

Actuation mechanism

To the best of our knowledge, the tensile stroke achieved in this study is far larger than that of the previously reported artificial muscles (**Figure 5A**). Furthermore, it is more than 3 times higher than the largest stroke reported so far, which results from hair artificial muscles prepared through disulfide cross-linking (3000%)[20]. Simply by twist insertion, coiling and steaming, hair artificial muscles with extremely large contraction or elongation stroke could be obtained.

It is known that the actuation mechanism of the twisted fiber based artificial muscles is muscle untwisting driven by the volume change, which arises from their response to external stimuli[1]. Moreover, by transforming the twisted fibers into coiled muscles, the untwisting torque derived torsional actuation upon external

stimulus can be translated into tensile actuation[4, 6]. Hair is one of the most important natural keratinous fibers based on α-keratin[24]. The stability of the keratin is maintained by intramolecular hydrogen bonds, making it susceptible to the ambient water content[25].

The structural change of the hair after treatment was characterized by DSC analysis. As shown in **Figure 5B** , in spite of the peak at around 230 that generally depicts the melting of the α-form crystallites, another peak at around 239 appeared on the DSC curve of the steamed hair. This endothermic event indicated the irreversible denaturation of α-keratin caused by steaming. Interestingly, no obvious peak showed at around 239 on the DSC curve of the heat hair, suggesting the important role of water vapor. It might be inferred that the intramolecular hydrogen bonds of the keratin were interfered with the ambient water vapor during the steaming process. Moreover, when the hair artificial muscle was immersed into water, the hydrogen bonds tended to rearrange, thus leading to the contraction or elongation of the artificial muscle. When the wet hair muscle was immersed in ethanol, it would dehydrate quickly and recover. Furthermore, torsional tethering is not required here to preserve the twist in the hair fibers.

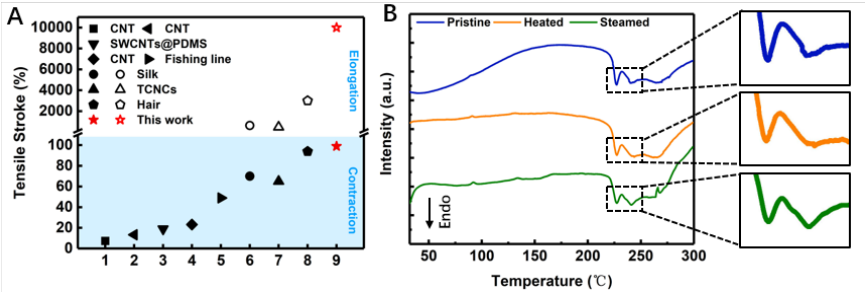

Figure 5 (A) Comparison of the tensile strokes between different artificial muscles[5, 8, 9, 12, 19-21, 23].**(B)** Differential scanning curves (DSCs) of the pristine hair, hair treated with only heat and with steam. Right panels magnified the events in the dashed boxes.

Reversibility and the long-term stability of the hair artificial muscles

To investigate the reversibility of the hair artificial muscles, 100 fully reversible water-ethanol stimulation cycles were demonstrated. The homochiral hair muscles contracted in water and re-elongated in ethanol, while the heterochiral hair muscles elongated in water and re-contracted in ethanol. This water and ethanol stimulation cycle is called a reversibility cycle and can be repeated many times. As shown in**Figure 6A** , after 100 water-ethanol stimulation cycles, the homochiral hair muscle could still contract to a short spring in 21 s in response to water and re-elongate to 100 times its initial length in ethanol, while the heterochiral hair muscle could elongate to 100 times its initial length in 40 s in response to water and re-contract to a short spring in only 25 s in ethanol. The change of the tensile stroke for both the homochiral and heterochiral hair muscles during the 100 reversible cycles is shown in **Figure 6B** and**Figure 6C** . It can be seen that there is no significant performance decrease, indicating the reversibility for both the homochiral and heterochiral hair artificial muscles.

Moreover, the long-term stability of the hair muscles was also studied.**Figure 6D** shows the function of the tensile stroke against time for a homochiral hair muscle with the diameter of 8 mm and twist density of 2650 turns m^{-1} after placing in ambient environment for 5 months. The hair muscle responded to both the water and ethanol stimulation and achieved a tensile stroke as large as 10000% within 30 s. The response rate shown in **Figure6F** exhibits that both the maximum contraction speed in water and the maximum elongation speed in ethanol could be over 1000% per second. Apart from the homochiral hair artificial muscles, the actuation of a heterochiral hair muscle with the diameter of 8 mm and twist density of 2650 turns m^{-1} after 5 months was also investigated. It can be seen from **Figure 6E** and**Figure 6G** that the

tensile stroke in response to water was also 10000% and the maximum actuation rate could be over 800% per second. These results demonstrated the excellent actuation performance of both the homochiral and heterochiral hair artificial muscles after 5 months, indicating their good long-term stability.

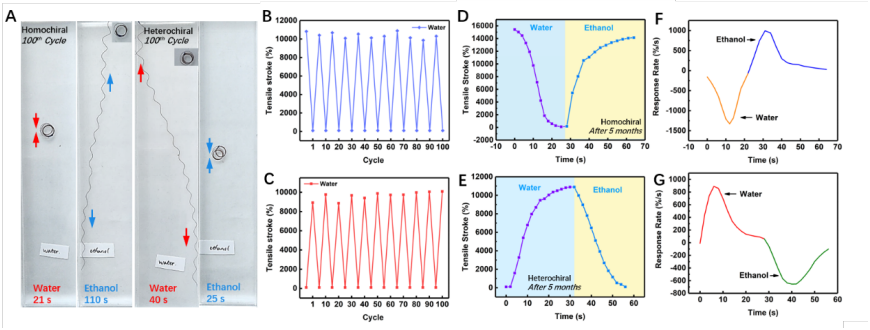

Figure 6 Characterization of the long-term stability of the hair artificial muscles. **(A)** Photographs of the homochiral and heterochiral artificial muscles before and after actuation in water and ethanol after 100 cycles. Tensile stroke of **(B)** the homochiral and **(C)** the heterochiral artificial muscles before and after actuation in water at 10 testing points (1, 10, 20, 30, 40, 50, 60, 70, 80, 90, 100). Tensile stroke of **(D)** a homochiral and**(E)** a heterochiral artificial muscle in response to water and ethanol after 5 months. The response rate of **(F)** the homochiral and **(G)** the heterochiral hair muscle to water and ethanol after 5 months.

Applications of the hair artificial muscles

The extremely large tensile stroke upon water stimulation and its fast recovery in ethanol makes the hair artificial muscle suitable for various applications. **Figure 7** displays several different application scenarios. First of all, a robotic "sea cucumber" that could climb long distances based on the heterochiral hair muscle with the spring index of 15 and the twist density of 2500 turns m^{-1} was made. The sea cucumber could crawl on a barbed plastic cord as long 200 mm by exchanging the water and ethanol stimulation two times (**Figure 7A**). The barbs on the surface of the cord all tilted in one direction, thus guiding the sea cucumber to move in the fixed direction.

Next, the energy generated from the water actuation of the homochiral hair muscle was used to pull a wheel model (˜2.8 g). The wheel model could move 40 mm within 143 s as the homochiral hair muscle contracted in response to water (**Figure 7B**). This result revealed that the homochiral hair muscle could work as an engine to actuate the movement of a wheel model which was approximately 500 times heavier than itself.

As shown in **Figure 7C** (**Video S5**), a single 97-mm-long homochiral hair artificial muscle was able to lift a weight 10 times heavier than itself by 57 mm (59% strain) in response to water in 60 s. The contractile work generated by the hair muscle during weight lifting normalized to the total weight of the muscle was considered the work capacity of the hair muscle. It was 5.38 J $kg^{-1}$for the homochiral hair muscle with the spring index of 8 and the twist density of 2500 turns m^{-1}.

The extremely large tensile stroke of the homochiral hair muscle upon water actuation indicates high sensitivity of the hair muscle to water, which could be used for smart switches. As illustrated in**Figure 7D** , two homochiral hair muscles were bound to the switch of a circuit. When the environment is dry, the circuit was connected and the LED light was on. However, when water appeared in the ambient environment and contacted the hair muscles, they would contract and disconnect the circuit, thus turning off the LED light. Photos in**Figure 7E** (**Video S6**) showed the smart switch turned off the LED light when the homochiral hair muscle contacted with water.

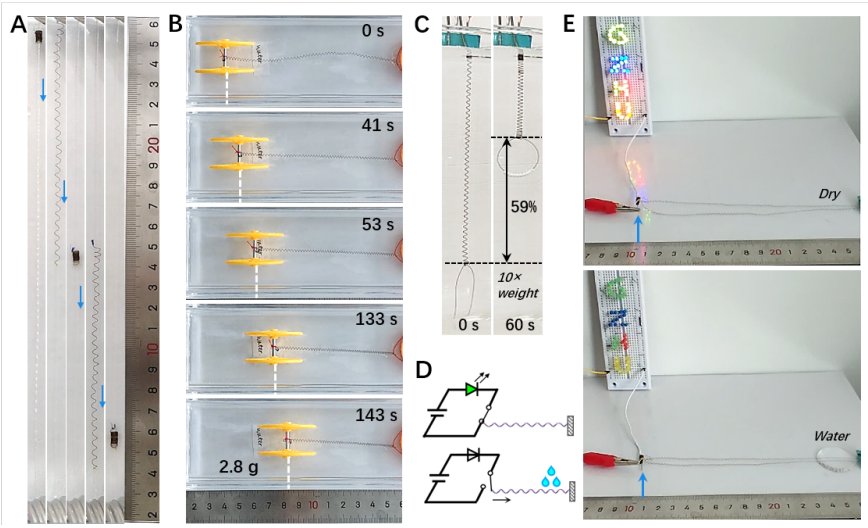

Figure 7 Applications of the hair artificial muscles.**(A)** Sequential photos showing a heterochiral hair muscle based "sea cucumber" crawling on a barbed wire under water and ethanol actuation. **(B)** Movement of the wheel model caused by the actuation of the homochiral hair artificial muscle in response to water.**(C)** Actuation of a homochiral artificial muscle in response to water lifting a weight 10 times its own weight by 59% in 60 s.**(D)** Schematic illustration of the circuit diagram for the smart switch based on the actuation of the homochiral hair muscle by water.**(E)** Photos showing the hair muscle switching off the LED light after contacting water.

Conclusion

In this study, tether-free hair artificial muscles with extremely large tensile stroke and fast recovery were successfully made through twist insertion, coiling and steaming, without any chemical crosslinking. Coiling the twisted hair fiber with large diameters increases the muscles' tensile stroke, and ethanol stimulation enables their fast recovery. The tensile stroke upon water actuation could be as large as 10000%, three times larger than the largest tensile stroke reported so far[20]. The fastest actuated muscle could fully recover in 10 to 20 seconds. Various applications such as long-distance climbing robots, weight pulling or lifting, and a smart water-sensitive switch were also demonstrated. This study provides a facile and green strategy to prepare advanced natural fiber-based artificial muscles, which have promising applications in soft robotics and biomedical fields.

Acknowledgement

This work was supported by the National Natural Science Foundation of China (grant no. 62002079, 62172114, 61772376, 62072129 and 62202112) and the National Key R&D Program of China (Grant no. 2019YFA0706401). The authors would like to thank Shiyanjia Lab (*www.shiyanjia.com*) for the support of DSC analysis.

Conflicts of interest

None.

Author contributions

The fabrication and characterization of the hair artificial muscles were carried out by Qian-Ru Xiao. The project was designed and performed by Si Sun, Xiao-Li Qiang and Xiao-Long Shi. The schematic illustrations for hair artificial muscles were prepared by Peng Xu. Qian-Ru Xiao and Si Sun prepared the manuscript. Xiao-Li Qiang and Xiao-Long Shi revised the manuscript. All authors commented on the manuscript.

Data availability statement

The data that support the findings of this study are available from the corresponding author upon reasonable request.

References

1 S. M. Mirvakili and I. W. Hunter, *Advanced Materials*2018**, 30** (6), 28.

2 Z. M. Hu, Y. L. Li, T. H. Zhao and J. A. Lv, *Applied Materials Today* 2022**, 27** , 101449.

3 Z. Liu, R. Zhang, Y. Xiao, J. Li, W. Chang, D. Qian and Z. Liu,*Materials Horizons* 2021**, 8** (6), 1783-1794.

4 X. Q. Leng, X. Y. Hu, W. B. Zhao, B. G. An, X. Zhou and Z. F. Liu,*Advanced Intelligent Systems* 2021**, 3** (5), 13.

5 R. Wang, Y. Shen, D. Qian, J. Sun, X. Zhou, W. Wang and Z. Liu,*Materials Horizons* 2020**, 7** (12), 3305-3315.

6 S. Aziz and G. M. Spinks, *Materials Horizons* 2020**,7** (3), 667-693.

7 J. Yuan, W. Neri, C. Zakri, P. Merzeau, K. Kratz, A. Lendlein and P. Poulin, *Science* 2019**, 365** (6449), 155-158.

8 Y. Cui, D. Li, C. Gong and C. Chang, *ACS Nano* 2021**,15** (8), 13712-13720.

9 K. Jin, S. Zhang, S. Zhou, J. Qiao, Y. Song, J. Di, D. Zhang and Q. Li, *Nanoscale* 2018**, 10** (17), 8180-8186.

10 J. Di, S. Fang, F. A. Moura, D. S. Galvao, J. Bykova, A. Aliev, M. J. de Andrade, X. Lepro, N. Li, C. Haines, R. Ovalle-Robles, D. Qian and R. H. Baughman, *Advanced Materials* 2016**, 28** (31), 6598-6605.

11 J. Foroughi, G. M. Spinks, G. G. Wallace, J. Oh, M. E. Kozlov, S. Fang, T. Mirfakhrai, J. D. W. Madden, M. K. Shin, S. J. Kim and R. H. Baughman, *Science* 2011**, 334** (6055), 494-497.

12 M. D. Lima, N. Li, M. J. de Andrade, S. Fang, J. Oh, G. M. Spinks, M. E. Kozlov, C. S. Haines, D. Suh, J. Foroughi, S. J. Kim, Y. Chen, T. Ware, M. K. Shin, L. D. Machado, A. F. Fonseca, J. D. W. Madden, W. E. Voit, D. S. Galvao and R. H. Baughman, *Science* 2012**,338** (6109), 928-932.

13 R. Cruz Silva, A. Morelos Gomez, H. Kim, H. Jang, F. Tristan, S. VegaDiaz, L. P. Rajukumar, A. L. Elias, N. Perea Lopez, J. Suhr, M. Endo and M. Terrones, *ACS Nano* 2014**, 8** (6), 5959-5967.

14 B. Fang, Y. Xiao, Z. Xu, D. Chang, B. Wang, W. Gao and C. Gao,*Materials Horizons* 2019**, 6** (6), 1207-1214.

15 C. Lang, E. C. Lloyd, K. E. Matuszewski, Y. Xu, V. Ganesan, R. Huang, M. Kumar and R. J. Hickey, *Nature Nanotechnology* 2022.

16 T. Mirfakhrai, J. D. W. Madden and R. H. Baughman, *Materials Today* 2007**, 10** (4), 30-38.

17 Y. Dou, Z. P. Wang, W. He, T. Jia, Z. Liu, P. Sun, K. Wen, E. Gao, X. Zhou, X. Hu, J. Li, S. Fang, D. Qian and Z. Liu, *Nature Communications* 2019**, 10** .

18 D. Liu, A. Tarakanova, C. C. Hsu, M. Yu, S. Zheng, L. Yu, J. Liu, Y. He, D. J. Dunstan and M. J. Buehler, *Science Advances*2019**, 5** (3).

19 T. Jia, Y. Wang, Y. Dou, Y. Li, M. J. de Andrade, R. Wang, S. Fang, J. Li, Z. Yu, R. Qiao, Z. Liu, Y. Cheng, Y. Su, M. Minary-Jolandan, R. H. Baughman, D. Qian and Z. Liu, *Advanced Functional Materials*2019**, 29** (18).

20 X. Leng, X. Zhou, J. Liu, Y. Xiao, J. Sun, Y. Li and Z. Liu,*Materials Horizons* 2021**, 8** (5), 1538-1546.

21 L. Dong, M. Ren, Y. Wang, J. Qiao, Y. Wu, J. He, X. Wei, J. Di and Q. Li, *Materials Horizons* 2021**, 8** (9), 2541-2552.

22 J. Deng, Y. Xu, S. He, P. Chen, L. Bao, Y. Hu, B. Wang, X. Sun and H. Peng, *Nature Protocols* 2017**, 12** (7), 1349-1358.

23 C. S. Haines, M. D. Lima, N. Li, G. M. Spinks, J. Foroughi, J. D. W. Madden, S. H. Kim, S. Fang, M. J. de Andrade, F. Goktepe, O. Goktepe, S. M. Mirvakili, S. Naficy, X. Lepro, J. Oh, M. E. Kozlov, S. J. Kim, X. Xu, B. J. Swedlove, G. G. Wallace and R. H. Baughman, *Science*2014**, 343** (6173), 868-872.

24 B. Wang, W. Yang, J. McKittrick and M. A. Meyers, *Progress in Materials Science* 2016**, 76** , 229-318.

25 E. Renuart and C. Viney, Biological fibrous materials: Self-assembled structures and optimised properties. In *Structural Biological Materials (Edited by M. Elices), Pergamon/Elsevier Science, Oxford* , 2000; pp 221-267.

Consent Statement

I, Qian-Ru Xiao, provided the hair samples and I have no objection to the hair being used in this study.

Supporting Information

Extremely large-stroke hair artificial muscles with fast recovery prepared by a facile and green method

Qian-Ru Xiao, Peng Xu, Si Sun, * Xiao-Li Qiang* and Xiao-Long Shi *

Video S1 Actuation of the homochiral hair artificial muscles in water.

Hosted file

`homochiral water.mp4` available at https://authorea.com/users/574061/articles/618104-extremely-large-stroke-hair-artificial-muscles-with-fast-recovery-prepared-by-a-facile-and-green-method

Video S2 Recovery of the homochiral hair artificial muscles in ethanol.

Hosted file

`homochiral ethanol.mp4` available at https://authorea.com/users/574061/articles/618104-extremely-large-stroke-hair-artificial-muscles-with-fast-recovery-prepared-by-a-facile-and-green-method

Video S3 Actuation of the heterochiral hair artificial muscles in water.

Hosted file

heterochiral water.mp4 available at https://authorea.com/users/574061/articles/618104-extremely-large-stroke-hair-artificial-muscles-with-fast-recovery-prepared-by-a-facile-and-green-method

Video S4 Recovery of the heterochiral hair artificial muscles in ethanol.

Hosted file

heterochiral ethanol.mp4 available at https://authorea.com/users/574061/articles/618104-extremely-large-stroke-hair-artificial-muscles-with-fast-recovery-prepared-by-a-facile-and-green-method

Video S5 Weight lifting of the homochiral hair artificial muscles in water.

Hosted file

weight lifting.mp4 available at https://authorea.com/users/574061/articles/618104-extremely-large-stroke-hair-artificial-muscles-with-fast-recovery-prepared-by-a-facile-and-green-method

Video S6 Smart switch based on the homochiral hair artificial muscles in response to water.

Hosted file

smart switch.mp4 available at https://authorea.com/users/574061/articles/618104-extremely-large-stroke-hair-artificial-muscles-with-fast-recovery-prepared-by-a-facile-and-green-method